

## *International Journal of Scientific Research and Reviews*

### **Photocatalytic Degradation of Methylene Blue Dye using $\text{CuBi}_2\text{O}_4$ Nanocatalyst and Effect of Various Operational Parameters.**

**Ch Jagadeesh<sup>1</sup> and B.B.V Sailaja<sup>1\*</sup>**

<sup>1</sup>Department of Inorganic and Analytical Chemistry, Andhra University,  
Visakhapatnam-530003, INDIA.

#### **ABSTRACT**

New visible-light responsive  $\text{CuBi}_2\text{O}_4$  nano particles (NPs) have been successfully synthesized by Co-precipitation method at 300 °C. The photo catalytic degradation of Methylene Blue (MB) dye has been investigated using  $\text{CuBi}_2\text{O}_4$  (NPs) as photo catalyst.  $\text{CuBi}_2\text{O}_4$  nano catalyst was found to be efficient catalyst for the degradation of dye and 92% degradation was observed in 120 min. Effect of various operational parameters such as amount of catalyst (0.1–0.25 g/L), concentration of dye (5 ppm–20 ppm) and pH (3–11) of dye solution on the rate of dye degradation was studied. The optimum operational parameters for the degradation of MB were observed at pH 10, at 10 ppm concentration and at a catalyst loading of 1 g/L. Moreover, hydroxyl radicals have been detected in the photo catalytic reaction mixture by using Terephthalic acid photoluminescence probing technique. The structural and morphological studies were carried out by using X-ray diffraction (XRD), Scanning Electron Microscope (SEM), Energy Dispersive Spectroscopy (EDS) and Fourier Transform Infrared (FT-IR) spectra showing the single phase monoclinic structure. The X-ray diffraction (XRD) analysis confirmed a single phase monoclinic crystal. The EDS plots revealed existence of no extra peaks other than constituents of the taken up composition.

**KEY WORDS:** Photo catalysis, Methylene Blue (MB),  $\text{CuBi}_2\text{O}_4$ , Terephthalic acid.

#### **\*Corresponding author**

**Dr.B.B.V. Sailaja**

Department of Inorganic and Analytical Chemistry,  
Andhra University,  
Visakhapatnam -530 003, INDIA.

Email: [sailajabbv.chem@gmail.com](mailto:sailajabbv.chem@gmail.com) , Mob No – +91-9441328956.

## **INTRODUCTION**

Heterogeneous photo catalysis has been widely investigated for the abatement of several toxic organic pollutants because of its ability to completely mineralize hazardous organic contaminants into harmless products at ambient temperature <sup>1</sup>. TiO<sub>2</sub> is used extensively as a photo catalyst because it is inexpensive, easy to synthesize, non-toxic, chemically inert, and highly photo stable. But, the wide band gap of TiO<sub>2</sub> restricts its absorption to U.V region with  $\lambda < 380\text{nm}$  which require substantial electrical input. Terrestrial solar radiation is composed of 4% U.V radiation, 52% visible light and 44% near infrared light. In order to exploit the large component of solar radiation, it is essential that the photo catalyst needs to be visible light responsive. Different strategies have been demonstrated to extend photo response of TiO<sub>2</sub> into visible light through (i) doping of metal atoms/anions and/or cations, (ii) surface sensitization with dyes, phthalocyanins, porphyrins and (iii) fabrication of nano composites with higher surface to volume ratio. Simultaneous research on ternary metal oxides as potential photo catalysts led to the development of ZnWO<sub>4</sub> <sup>2</sup>, CaBi<sub>2</sub>O<sub>4</sub> <sup>3</sup>, BaBiO<sub>3</sub> <sup>4</sup>, BiVO<sub>4</sub> <sup>5</sup>, Bi<sub>2</sub>WO<sub>6</sub> <sup>3</sup>, Bi<sub>2</sub>MoO<sub>6</sub> <sup>4</sup>, Bi<sub>2</sub>Mo<sub>2</sub>O<sub>9</sub> <sup>5</sup>, Bi<sub>2</sub>Mo<sub>3</sub>O<sub>12</sub> <sup>6</sup>, Fe<sub>2</sub>Mo<sub>3</sub>O<sub>12</sub> <sup>7</sup>, NaBiO<sub>3</sub> <sup>8</sup>, FeV<sub>3</sub>O<sub>8</sub> <sup>9</sup> etc. as potential photo catalysts for degradation of dyes and other aromatic pollutants. Majority of these visible light active photo catalysts contain Bi as one of the components. Binary metal oxide systems Bi<sub>2</sub>O<sub>3</sub>-V<sub>2</sub>O<sub>5</sub>, Bi<sub>2</sub>O<sub>3</sub>-MoO<sub>3</sub> and Bi<sub>2</sub>O<sub>3</sub>-WO<sub>3</sub> form a large group of visible light responsive photo catalysts, probably due to the valance band formed from Bi (6s) and O (2p) orbital's resulting in a smaller band gap <sup>10</sup>. The light absorption property of the photo catalyst plays an important role in its photo catalytic efficiency. Bismuth oxide (Bi<sub>2</sub>O<sub>3</sub>) is recently an attractive material due to its good electrical conductivity, thermal properties, and narrow band-gap (2.8 eV). Up to now, Bi<sub>2</sub>O<sub>3</sub> has been prepared by different methods with various morphologies and properties, such nano rod, nano particle, microsphere, nano fiber <sup>11,12,13</sup>. 3-D flowerlike Bi<sub>2</sub>O<sub>3</sub> fabricated by a hydrothermal method and Tseng et al. <sup>14</sup> have also prepared hierarchical bismuth oxide architectures via a solution precipitation.

Synthetic dyes are a major part of our life, including methylene blue as they are found in various products ranging from clothes to leather, accessories to furniture. The unfavorable side effect of their extensive use is the fact that up to 12% of these dyes are wasted during the dyeing process, and that approximately 20% of this wastage enters the environment (mostly in the water supply) <sup>17</sup>.

The molecular formula of a heterocyclic aromatic chemical compound methylene blue is C<sub>16</sub>H<sub>18</sub>N<sub>3</sub>SCl. At room temperature it appears as a solid, odorless, dark green powder that yields a blue solution when dissolved in water. It has many uses in a variety of diverse fields of studies, such as chemistry and biology. In analytical chemistry methylene blue is widely used as a redox indicator. Solutions of this substance will turn colorless if exposed to easily oxidized substances otherwise they

are blue when in reducing environment. Its chemical structure is given below. These dyes have to be removed before discharge into water bodies<sup>18,19,20,21</sup>. Methylene blue is widely used in industries, for temporary hair colorant, coloring papers, dyeing cotton, wools and coating for paper stock. Severe exposure to methylene blue will cause health problems when the dose is above 2 mg/kg such as increased heart rate, vomiting, shock, Heinz body formation, and cyanosis and tissue necrosis in humans<sup>22</sup>. MB doses exceeding 2 mg/kg, may cause or can cause toxicity in high doses. The features of toxicity being cardiac arrhythmias, coronary vasoconstriction, decreased cardiac output, renal blood flow and mesenteric blood flow; increased pulmonary vascular pressure & pulmonary vascular resistance and gas exchange deterioration and precipitate serious serotonin toxicity and discoloration of urine and bladder irritation (doses over 80 µg)<sup>23</sup>. The molecular structure of MB shown in Fig. 1.

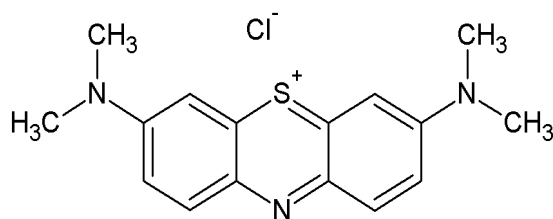


FIG 1. Structure of Methylene Blue

## MATERIALS AND METHODS

### *Synthesis of photo catalyst:*

CuBi<sub>2</sub>O<sub>4</sub> NPs were prepared by co-precipitation route at 300 °C. In the preparation stoichiometric amounts (1:2 ratio) of Cu(NO<sub>3</sub>)<sub>2</sub>·3H<sub>2</sub>O (LOBA CHEMIE PVT. Ltd) and Bi(NO<sub>3</sub>)<sub>3</sub>·5H<sub>2</sub>O (98% HIMEDIA) were dissolved in Ethylene Glycol (98% HIMEDIA) separately by using magnetic stirrer. After completion of solubility two solutions were mixed with each other and heated at 50 °C. By maintaining this temperature, 5N NaOH (98% HIMEDIA) was added to maintain the p<sup>H</sup> at 8.5. At this p<sup>H</sup> the mixed precursors start react with each other to produce precipitate. This precipitate was washed several times with distilled water to completely remove the excess NaOH and the precipitate was filtered and dried at 80 °C in an air oven. The dried powder was claimed at 300 °C. The resultant catalyst was grounded to several hours to get fine powder and subjected to phase identification, micro structural investigation and photo catalytic studies.

### *Characterization techniques:*

Phase purity of the resultant powder was investigated with X-ray diffractometer (PANalytical-X<sup>PERT</sup> PRO, Japan) at room temperature, using Nickel filtered Cu-K $\alpha$  radiation ( $\lambda = 1.54059 \text{ \AA}$ ), with a scan rate of 2° min<sup>-1</sup>. Micro structural investigation of the sample was performed on the

powdered sample using SEM (JEOL-JSM-6610LV, Tokyo, Japan). UV-visible diffuse reflectance spectrum (UVDRS) of the sample was obtained with dry pressed disk samples using Shimadzu UV-visible spectrophotometer (UV-3600) between 200 to 800 nm range. Spectral grade BaSO<sub>4</sub> was taken as reference in the UV-DRS.

#### ***Photo catalytic studies:***

Photo catalytic activity of CuBi<sub>2</sub>O<sub>4</sub> was evaluated in terms of degradation of MB dye under visible light. 0.05 gm, 0.1 gm, 0.15 gm, 0.2 gm and 0.25 gm of the catalyst was dispersed separately in 100ml MB aqueous solution (10 mg/L) and the suspension was magnetically stirred for half an hour in dark to ensure adsorption/desorption equilibrium between photo catalyst powder and dye. The suspension was then exposed to 400 wt metal halide lamp; 5ml aliquots were pipetted at periodic time intervals and filtered through 0.45 micron Millipore filters to remove the suspended powder. The spectra as a function of irradiation time were recorded using UV-Visible spectrophotometer (Schimadzu). The extent of photo degradation was calculated using the following equation

$$\% \text{ Photo degradation} = [(A_0 - A_t) / A_0] \times 100$$

Where A<sub>0</sub> and A<sub>t</sub> correspond to the initial absorbance and absorbance at time “t” respectively.

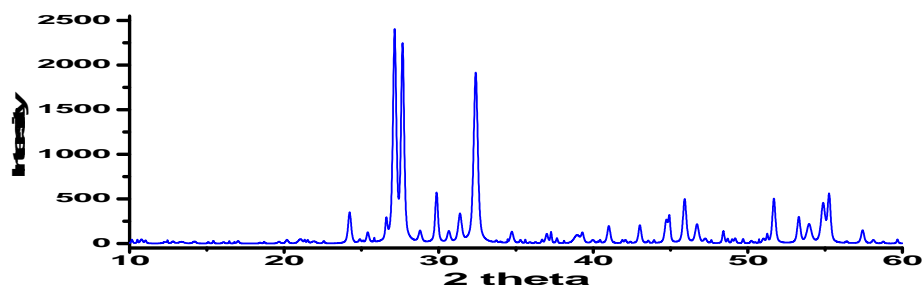
#### ***Photoluminescence studies:***

50 mg CuBi<sub>2</sub>O<sub>4</sub> catalyst is added to the beaker containing 100 ml of terephthalic acid (TPA) solution (0.25 mmol L<sup>-1</sup> in 1mmol L<sup>-1</sup> NaOH solution) and 10 μml H<sub>2</sub>O<sub>2</sub>. The solution is stirred for 15 min in dark followed by irradiation by 400 w metal halide lamp for 30 min. The reacted solution was centrifuged and the clear solution is used for photoluminescence measurements in a fluorescence spectrofluorometer (Fluoromax 4) with the excitation wavelength of 315 nm.

## **RESULTS AND DISCUSSION**

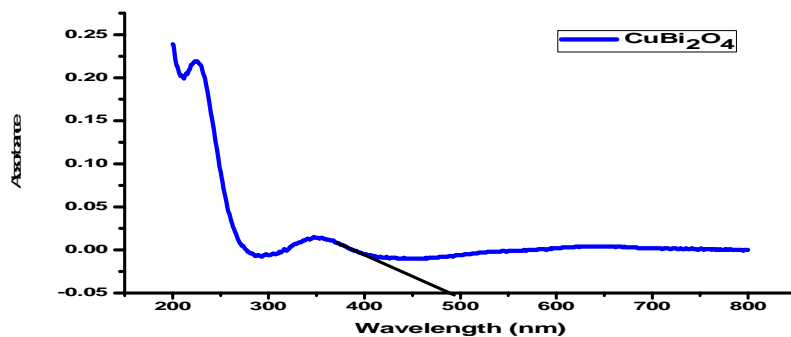
#### ***X-ray diffraction studies:***

The crystal structure and size of the obtained CuBi<sub>2</sub>O<sub>4</sub> was analyzed by X-ray diffraction. **Fig. 2** displays the XRD pattern of the sample. The XRD pattern of the CuBi<sub>2</sub>O<sub>4</sub> can be indexed with six CuBi<sub>2</sub>O<sub>4</sub> diffraction peaks at 27.8° (211), 29.6° (220), 33.1° (310), 44.9°(302), 46.5°(411), 52.71°(213) (JCPDS 72-0493), which suggests the presence of pure monoclinic phase of crystalline CuBi<sub>2</sub>O<sub>4</sub> in the sample. The main diffraction peaks were selected to calculate the average grain size of CuBi<sub>2</sub>O<sub>4</sub> by using the Scherrer's formula. The calculated average size of CuBi<sub>2</sub>O<sub>4</sub> nano particles by using Scherrer's formula (**Crystallite size Dp = K λ / (β cos Θ)**) observed is 68.29 nm.

FIG2. X-ray diffraction patterns of  $\text{CuBi}_2\text{O}_4$ .

### *UV–Vis diffuse reflectance studies:*

The UV–visible diffuse reflectance spectrum of  $\text{CuBi}_2\text{O}_4$  is shown in **Fig. 3**. It can be seen that the absorption wavelength edge of  $\text{CuBi}_2\text{O}_4$  is extended greatly toward visible light and its absorption intensity is also greatly increased.  $\text{CuBi}_2\text{O}_4$  has greater absorption in the wavelength range of 300–800 nm. This indicates that the prepared sample absorbs both UV and visible light quite well, which is better than that of  $\text{TiO}_2$ . So the formation rate of electron–hole pairs on the photo catalyst surface also increases greatly in visible light irradiation. As can be seen in Fig. 3, the as-synthesized  $\text{CuBi}_2\text{O}_4$  exhibits an absorption onset at 489.502333 nm, which corresponds to band gap energy of 2.61 eV. This value is much lower than that of  $\text{TiO}_2$  (3.2 eV) and thus the as synthesized  $\text{CuBi}_2\text{O}_4$  sample can be predicted to be a satisfying visible light active photo catalyst.

FIG 3. UV–Vis Diffuse Reflectance Spectra Of  $\text{CuBi}_2\text{O}_4$ 

### *Micro structural investigation studies:*

The microstructures of the obtained samples were studied by SEM analysis as can be seen from **Fig 4. a)** The SEM image shows that the photo catalyst consist of a large number of hierarchical nanostructures like submicro-flowers with the size less than 100 nanometers and two-dimensional crystalline nano particles. These particles exhibit agglomerated<sup>18</sup> morphology due to the ultrafine nature of the sample. EDS analysis of NPs shown in **Fig 4. b)**. It can be seen that the sample was composed of Bi, O elements and Cu respectively. The atomic percentages of Cu, Bi and

O in  $\text{CuBi}_2\text{O}_4$  are listed in **Table.1** according to the EDS data. The quantifications of Cu:Bi:O is 1:1.97:4.19. The atomic ratio of Cu:Bi:O is close to 1:2:4, which closely agrees with the stoichiometric composition of  $\text{CuBi}_2\text{O}_4$ <sup>18,19</sup>. This result is consistent with the XRD pattern presented above.

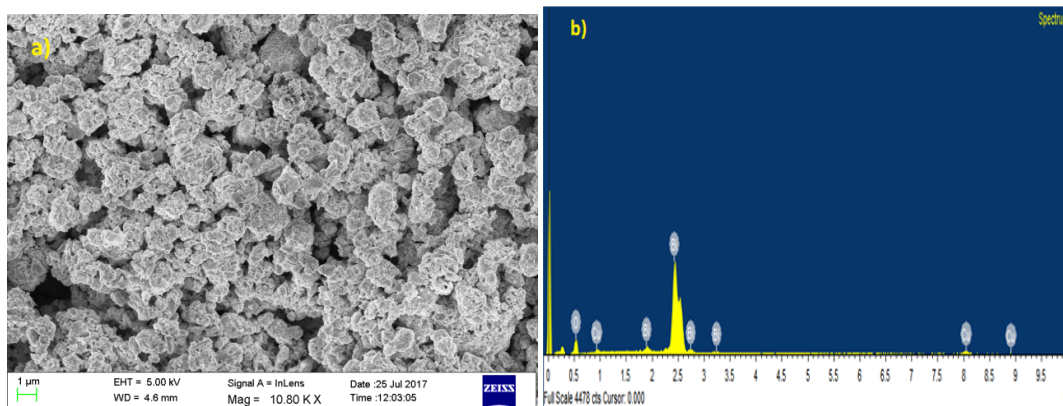


FIG 4. a) SEM image and b) EDS spectra of  $\text{CuBi}_2\text{O}_4$

Table.1. The atomic percentage (mol %) of Cu, Bi and O in  $\text{CuBi}_2\text{O}_4$ .

Compound	Cu	Bi	O	Atomic Ratio
$\text{CuBi}_2\text{O}_4$	13.95	27.53	58.52	1:1.97:4.19

**FT-IR studies:**

The IR spectra of the calcined powder of  $\text{CuBi}_2\text{O}_4$  shown in **Fig. 5**. After drying at 120°C, the spectrum is complex due to the existence of lots of organic compounds. The broad one around 700 ~ 400  $\text{cm}^{-1}$  originates from the metal-oxygen (Bi-O) vibration. The absorption band observed at 866  $\text{cm}^{-1}$  indicates the symmetric stretching of Bi-O bond in  $\text{CuBi}_2\text{O}_4$ <sup>20</sup>. Bending vibrations of Cu-O at 574.79<sup>21</sup> supports monoclinic structure of the catalyst. Stretching frequencies at 478.36 belongs to Cu-O<sup>21</sup>.

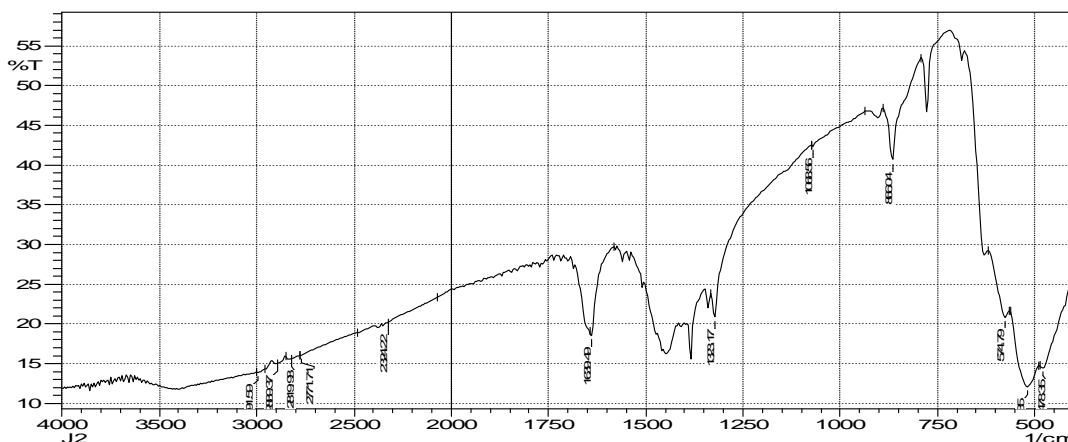


FIG 5. FT-IR spectrum of  $\text{CuBi}_2\text{O}_4$ .

### Photo catalytic Degradation Studies:

With the aim to show the effect of irradiation time on MB degradation, in the presence of  $\text{CuBi}_2\text{O}_4$ , the evolution of its visible absorption spectrum was monitored during 120 min. The samples were taken and analyzed periodically each 20 min. First, the solutions were stirred for approximately 30 min in the dark to sufficiently adsorb dye molecules, and then irradiated under a 400 W xenon lamp with a 420 nm cutoff filter and a 500 nm filter to assess the visible photo catalytic properties. The recorded absorption spectra are shown in **Fig.6**, which shows the process of MB dye degradation after exposure to visible light irradiation in the presence of  $\text{CuBi}_2\text{O}_4$  photo catalyst. The UV–visible absorption spectrum shows a peak at 664 nm. When irradiation time was increased, the absorption intensity of the peak at 664 nm decreased, which confirms the progress of the degradation of the MB dye used as a synthesized photo catalyst. For the  $\text{CuBi}_2\text{O}_4$  photo catalyst, 94% degradation of the MB dye took only 120 min.

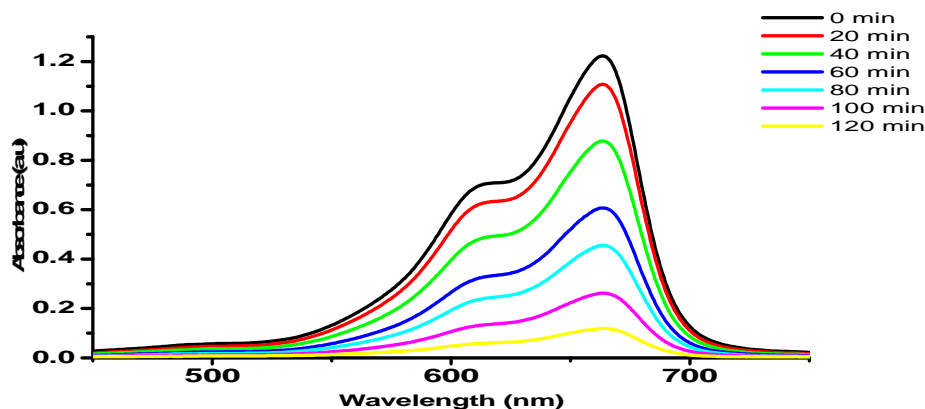
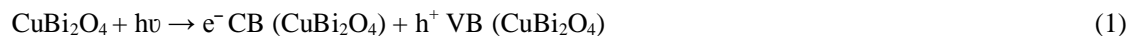


FIG6. Photo catalytic degradation of MB over  $\text{CuBi}_2\text{O}_4$ .

The mechanism can be predicted by the following equations <sup>22</sup>. Possible photo catalytic mechanism involved is suggested as follows;



### Photoluminescence Studies:

Rapid formation of  $\cdot\text{OH}$  free radicals through steps (3) and (4) is the important in accumulation of more  $\cdot\text{OH}$  free radicals which used for disintegration of MB. In order to confirm the generation  $\cdot\text{OH}$  free radicals during irradiation of  $\text{CuBi}_2\text{O}_4$ , photoluminescence spectroscopy was

used with Terephthalic acid (TPA) as a probe molecule. TPA combines preferentially with  $\cdot\text{OH}$  to form hydroxyl terephthalic acid (HTPA) which shows a characteristic luminescence peak at 422 nm. Fig7. depicts photoluminescence spectra for  $\text{CuBi}_2\text{O}_4 + \text{TPA}$  prior to and after irradiation. Intense luminescence peak after irradiation confirms formation of  $\cdot\text{OH}$  free radicals due to irradiation.

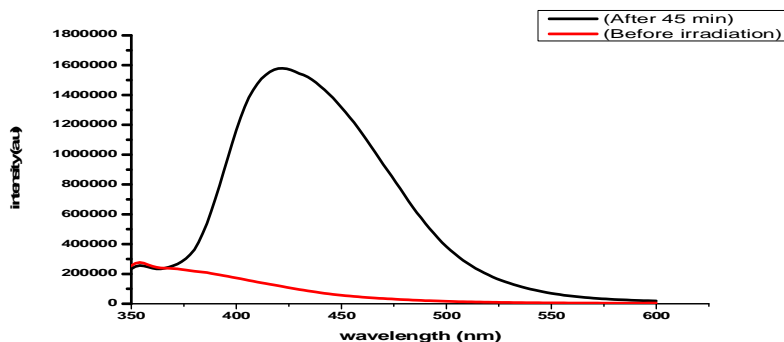


FIG 7. Photoluminescence spectra for  $\text{CuBi}_2\text{O}_4 + \text{TPA}$  prior to and after irradiation for 45 minutes.

## OPERATIONAL PARAMETERS

### Effects of pH variation:

At different pH values, percentage degradation of MB as a function of time is shown in Fig 8. and effect of variation of pH on reaction rate shown in table 2 and Fig 9.

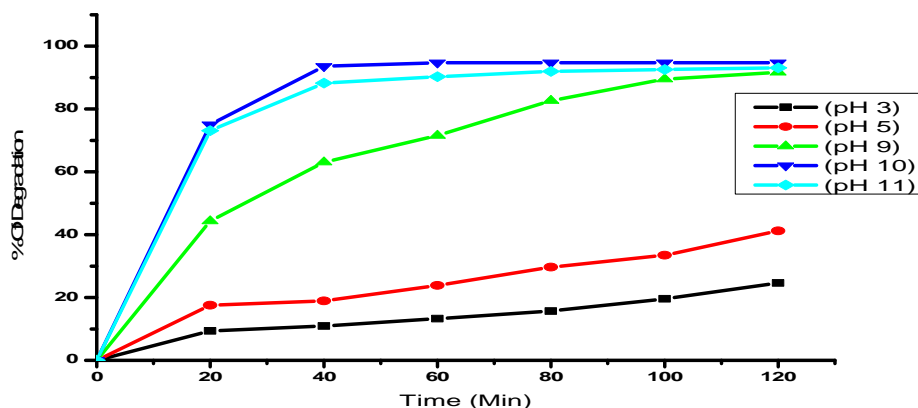


FIG 8. Effect of pH of solution on the photo catalytic Activity of  $\text{CuBi}_2\text{O}_4$  Photo catalyst on the % degradation of MB. here catalyst dosage = 0.10 g,  $[\text{MB}] = 10 \text{ ppm}$ .



Table 2. Effect of variation of pH on reaction rate

Effects of Variation of pH	CuBi <sub>2</sub> O <sub>4</sub> = 0.1 g Temp = 308 k Rate mgL <sup>-1</sup> min <sup>-1</sup>
pH	
3.0	0.18
5.0	0.15
9.0	2.1
10	2.35
11	1.78

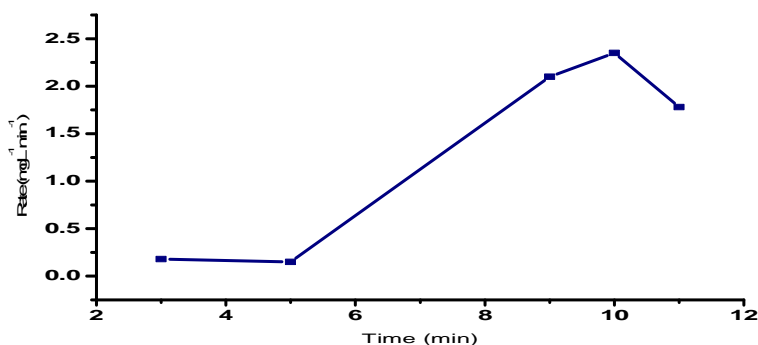


FIG 9. Effect of variation of pH on reaction rate

It is known that semiconductor metal oxide particles dispersed in water behave like diprotic acids in this regard for CuBi<sub>2</sub>O<sub>4</sub>, the hydroxyl group undergoes acid/ base equilibria<sup>29</sup> moreover Tang et al.,<sup>30</sup> for charged substrates, there is a significant dependency on pH value for the photocatalytic degradation, since the overall surface charge on the catalyst and the adsorptive properties of CuBi<sub>2</sub>O<sub>4</sub> nonmaterial depend strongly on solution pH. Since MB is cationic dye in aqueous solution and in basic pH, the surface of the catalyst attains negative charge, there would be an electrostatic attraction which would speed up the degradation percentage because excess OH<sup>-</sup> anions which facilitate photo generation of hydroxyl radicals and it reaches a maximum at pH 10<sup>31</sup>.

The dye solution was degraded and semi-conductor CuBi<sub>2</sub>O<sub>4</sub> dissolved in highly acidic media and therefore photocatalytic degradation could not be investigated at lower pH range. The rate constants (k) for this reaction were determined using the expression  $k=2.303 \times \text{Slope}$ . The results were reported in above table. The rate of the degradation of MB was found to increase with increase in the pH value of the medium. In alkaline medium there is a greater probability for the formation of hydroxyl radicals (OH<sup>·</sup>), which can act as oxidant. Thus the rate of the photocatalytic degradation of the dye increases. But after certain pH value 10 a further increase in pH of medium decreases the rate of photocatalytic degradation. It may be due to the fact that the dye does not remain in its cationic form. Due to greater concentration of OH<sup>-</sup> and as such the reaction rate decreases.

**Effect of amount of CuBi<sub>2</sub>O<sub>4</sub>:**

In order to recognize and identify the best concentration of CuBi<sub>2</sub>O<sub>4</sub> NPs, degradation experiments were carried out with MB under visible light irradiation. The rate of degradation of MB has been studied by the measurement of MB absorbance and the results are presented in Fig. 10, Table 3, and Fig. 11.

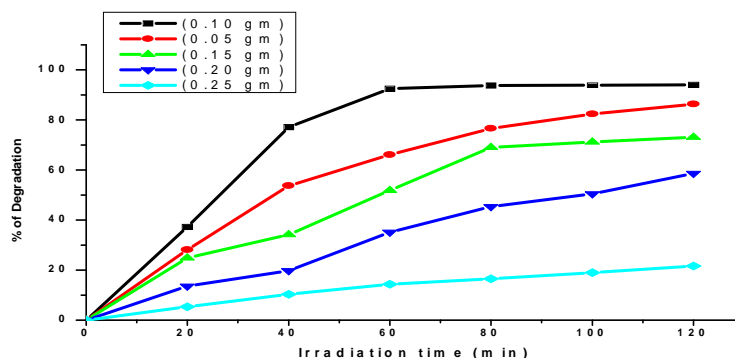


**FIG 10.** Effect of dopant concentration on the photo catalytic activity of CuBi<sub>2</sub>O<sub>4</sub> photo catalyst on the % degradation of MB. Here pH 10, [MB] = 10 ppm.

**Table.3** Effect of variation of amount of catalyst on reaction rate

pH = 10	[MB] = 10 ppm Temp = 308 k
Amount of CuBi <sub>2</sub> O <sub>4</sub> gm	Rate mgL <sup>-1</sup> min <sup>-1</sup>
0.05	1.45
0.1	1.65
0.15	0.93
0.2	0.77
0.25	0.27

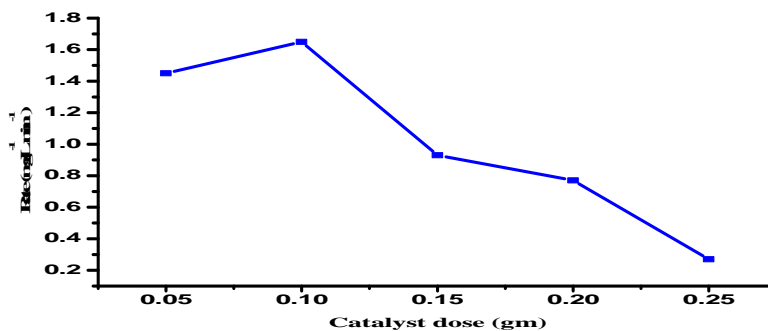


**FIG 11.** Effect of variation of amount of catalyst on reaction rate

The highest photo catalytic performance of the photo catalyst may be because of its narrowing band gap, less crystallite size and high surface area of CuBi<sub>2</sub>O<sub>4</sub>. As evident from the above data, the value of k increases with the increase in the amount of CuBi<sub>2</sub>O<sub>4</sub> but time taken for degradation of MB decreases with the increase in the amount of CuBi<sub>2</sub>O<sub>4</sub>. This increase in the rate

of degradation may be attributed to increase in the exposed surface area of the  $\text{CuBi}_2\text{O}_4$ . But after certain limit (0.1 g) if the amount of  $\text{CuBi}_2\text{O}_4$  is increased further, there will be no increase in the exposed surface area of the Photo catalyst. It may be considered like a saturation point, above which increase in the amount of  $\text{CuBi}_2\text{O}_4$  has no additional or negligible effect on the rate of photo catalytic degradation of MB.

**Effects of Methylene Blue concentration:**

The role of initial concentration of MB on the rate of degradation is illustrated in Fig. 12, Table 4, and Fig. 13. The influence of initial concentration of MB on the rate of degradation experiments was carried out from 5 ppm, 10ppm, 15 ppm and 20 ppm of dye, at a fixed amount of  $\text{CuBi}_2\text{O}_4$  photo catalyst as 0.10 gm, and pH of solution at 10.

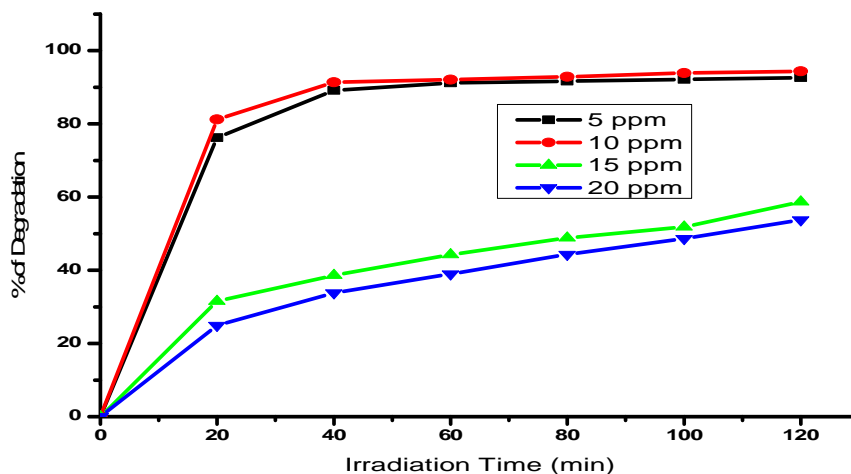


Fig 12.Effect of initial dye concentration on the photo catalytic activity of  $\text{CuBi}_2\text{O}$  photo catalyst on the % degradation of [MB]. Here catalyst dosage = 0.10 g, ph 10.

Table.4. Effect of variation of [MB] on reaction rate

pH = 10	$\text{CuBi}_2\text{O}_4 = 0.1 \text{ g}$ Temp = 308 k
[MB] in ppm	Rate $\text{mgL}^{-1}\text{min}^{-1}$
5	1.2
10	1.5
15	1.05
20	0.45

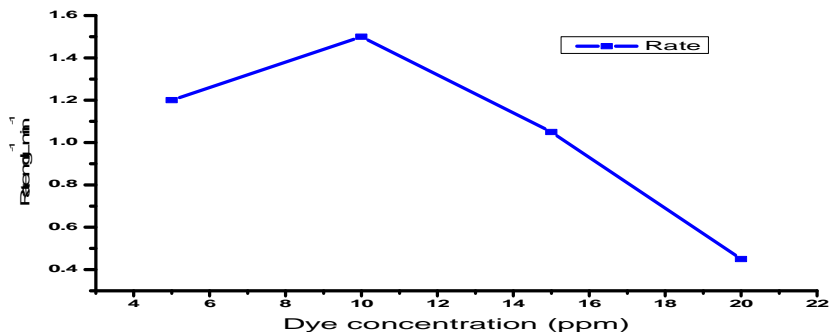


fig 13. Effect of variation of [MB] on reaction rate

Photo catalytic degradation increases with an increase in the concentration of dye up to 10 ppm. This may be due to the fact that as the concentration of the dye exceeds, more dye molecules will be available for excitation and energy transfer<sup>32,33</sup>. But beyond the optimum concentrations, the pollutant starts covering the surface of photo catalyst from light intensity<sup>34</sup>. Hence, there is a decrease in photo catalytic activity on the further pollutants concentration increase. It is evident from the data that with the increasing [MB], reaction rate increases due to the increase in number of molecules participating in the reaction but after the optimum value of concentration 10 ppm, the rate of the reaction decreases. It can be explained on the basis that as the concentration of the dye was increased, it may start acting like a filter for the incident light and does not allow light to reach the semi-conductor surface.

## CONCLUSION

Visible light assisted photo catalytic degradation of Methylene Blue was performed in the presence of the semiconductor  $\text{CuBi}_2\text{O}_4$ . The degradation rate increased with increasing pH because more hydroxyl ions were present (generating more hydroxyl radicals). It attains maximum rate at pH 10; a further increase in pH above 10 results in a decrease in the rate of the reaction, because of decreasing attraction between the neutral form of the dye and the negatively charged semiconductor surface. Increasing the concentration of MB also increased the rate up to a certain value due to the increase in the number of dye molecules, but it shows a declining behavior on further increase of the concentration of dye. This decrease may be attributed to the fact that at higher concentration, the dye may acts as an internal filter for the incident radiations, which decreases the intensity of the incident radiation on the semiconductor particles. The results indicate that initially the rate increases with increasing amount of semiconductor but after 0.10 g, the degradation rate decreases. This may be due to the complete coverage of the bottom of the reaction vessel by the semiconductor. Any further increase will not add to an increase in the exposed surface area but only increases the thickness of the

layer. An increase in the light intensity will increase the number of photons striking semiconductor  $\text{CuBi}_2\text{O}_4$  powder per unit area per second and as a consequence, the reaction rate increases almost linearly with the increase in light intensity. The optimum reaction conditions were obtained as: pH = 10; [Methylene Blue]= 10 ppm;  $\text{CuBi}_2\text{O}_4$ = 0.10 g. Formation of  $\cdot\text{OH}$  free radicals was confirmed by photoluminescence spectroscopy using Terephthalic acid. At these optimum parameters 94% of MB was degraded successfully within 120 minutes.

## **ACKNOWLEDGMENTS**

One of the authors (Ch.J) would like to thank University Grant Commission (UGC), New Delhi, INDIA, for the financial support of this research work through RGNF No. "F1-17.1/2016-17/RGNF-2015-17-SC-AND-6314/(SA-III/Website)"

## **REFERENCES**

1. Ahmed S, Rasul MG, Martens WN, Brown R, Hashib MA. et al. Advances in heterogeneous photocatalytic degradation of phenols and dyes in wastewater: A review. *Water Air Soil Pollut.* 2011; 215(1-4):3-29.
2. Montini T, Gombac V, Hameed A, Felisari L, Adami G, Fornasiero P. et al. Synthesis, characterization and photocatalytic performance of transition metal tungstates. *Chem Phys Lett.* 2010;498(1-3):113-119.
3. Tang J, Zou Z, Ye J. et al. Efficient photocatalytic decomposition of organic contaminants over  $\text{CaBi}_2\text{O}_4$  under visible-light irradiation. *Angew Chemie - Int Ed.* 2004; 43(34):4463-4466.
4. Tang J, Zou Z, Ye J. et al. Efficient photocatalysis on  $\text{BaBiO}_3$  driven by visible light. *J Phys Chem C.* 2007;111(34):12779-12785.
5. Martinez-de la Cruz A, Prez UMG. et al. Photocatalytic properties of  $\text{BiVO}_4$  prepared by the co-precipitation method: Degradation of rhodamine B and possible reaction mechanisms under visible irradiation. *Mater Res Bull.* 2010;45(2):135-141.
6. Liao Y-H Ben, Wang JX, Lin J-S, Chung W-H, Lin W-Y, Chen C-C. et al. Synthesis, photocatalytic activities and degradation mechanism of  $\text{Bi}_2\text{WO}_6$  toward crystal violet dye. *Catal Today.* 2011;174(1):148-159.
7. Martinez-de la Cruz A, Obregn Alfaro S. et al. Synthesis and characterization of  $\text{Bi}_2\text{MoO}_6$  prepared by co-precipitation: Photoassisted degradation of organic dyes under vis-irradiation. *J Mol Catal A Chem.* 2010;320(1-2):85-91.
8. Li H, Li K, Wang H. et al. Hydrothermal synthesis and photocatalytic properties of bismuth

- molybdate materials. *Mater Chem Phys*. 2009;116(1):134-142.
9. Rajesh B. et al. Rapid Photo Catalytic Degradation of Crystal Violet And Carmine Indigo Under Sun Light By  $\text{Fe}_2\text{Mo}_3\text{O}_{12}$ . 2014; 3(4):1670-1678.
  10. Chang X, Yu G, Huang J, et al. Enhancement of photocatalytic activity over  $\text{NaBiO}_3/\text{BiOCl}$  composite prepared by an in situ formation strategy. *Catal Today*. 2010;153(3-4):193-199.
  11. Zhang L, Zhou J, Zhang C. et al. pH-controlled growth of ultrathin iron vanadium oxide ( $\text{FeV}_3\text{O}_8$ ) nanoplatelets with high visible-light photo-catalytic activity. *J Mater Chem A*. 2014; (36):14903-14910.
  12. M. Oshikiri MB. et al. Water Molecule Adsorption Properties on the  $\text{BiVO}_4$  . Surface. *J Phys Chem B*. 2006; 110:9188–9194.
  13. Anandan S, Wu JJ. Microwave assisted rapid synthesis of  $\text{Bi}_2\text{O}_3$  short nanorods. *Mater Lett*. 2009; 63(27):2387-2389.
  14. Anandan S, Lee G, Chen P, Fan C, Wu JJ. et al. Removal of Orange II Dye in Water by Visible Light Assisted Photocatalytic Ozonation Using  $\text{Bi}_2\text{O}_3$  and Au /  $\text{Bi}_2\text{O}_3$  Nanorods. 2010; (38): 9729-9737.
  15. Hsieh SH, Lee GJ, Chen CY, et al. Synthesis of Pt Doped  $\text{Bi}_2\text{O}_3 / \text{RuO}_2$  Photocatalysts for Hydrogen Production from Water Splitting Using Visible Light. 2012; (76): 5930-5936.
  16. Tseng T, Choi J, Jung D, Davidson M, Holloway PH. et al. Hierarchical Architectures of Gamma-Phase. 2010; 9(4): 943-946.
  17. Sujith Alen , Vinodha S. et al. Studies on colour removal efficiency of textile dyeing waste water using Moringo Olifera. *SSRG International J. of Civil Engineering (SSRG-IJCE)* – 2014; **1(5)**:53-64.
  18. Shaul GM, Holdsworth TJ, Dempsey CR, et al. Fate of water soluble azo dyes in the activated sludge process. *Chemosphere*. 1991; 22:107-119.
  19. Banat IM, Nigam P, Singh D, Marchant R. et al. Microbial decolorization of textile-dye-containing effluents. 1997; 58(1996): 217-227.
  20. Robinson T, McMullan G, Marchant R, Nigam P. et al. Remediation of dyes in textile effluent : a critical review on current treatment technologies with a proposed alternative. 2001; 77: 247-255.
  21. Ali DM, Suresh A, Kumar RP, Gunasekaran M, Thajuddin N. Efficiency of Textile Dye Decolorization by Marine Cyanobacterium , *Oscillatoria formosa* NTDM02 mg / ml. 2011;3(1):9-13.
  22. Zollinger H., et al. Syntheses, Properties and Applications of Organic Dyes and Pigments. *Color Chemistry: VCH Publishers, Weinheim*, 1991; 3(5):144-158.

23. Ramsay RR., Dunford C., and Gillman C.K., et al. Methylene blue and serotonin toxicity: inhibition of monoamine oxidase A (MAO A) confirms a theoretical prediction. *Br. J. Pharmacol.*, 2007; **152 (6)** : 946-958.
24. Zhang J, Jiang Y, Gao W, Hao H. et al. Synthesis and visible photocatalytic activity of new photocatalyst  $\text{MBi}_2\text{O}_4$ (M=Cu, Zn). *J Mater Sci Mater Electron*. 2015;26(3):1866-1873.
25. Zhang J, Jiang Y. et al. Preparation, characterization and visible photocatalytic activity of  $\text{CuBi}_2\text{O}_4$  photocatalyst by a novel sol-gel method. *J Mater Sci Mater Electron*. 2015;26(6):4308-4312.
26. Varaprasad K, Ramam K, Siva G, Reddy M, Sadiku R, Varaprasad K. et al. Development and characterization of nano-multifunctional materials for advanced applications. 2014; 5(9):658-671.
27. Hosseini-Sarvari M, Moeini F. et al. Nano copper (i) oxide/zinc oxide catalyzed N-arylation of nitrogen-containing heterocycles with aryl halides and arylboronic acids in air. *RSC Adv*. 2014;4(14):7321-7329.
28. Umabala A.M, Suresh.P, AVPR. et al. Effective visible light photocatalytic degradation of Brilliant green using  $\text{H}_2\text{O}_2$  sensitized  $\text{BiVO}_4$ . *Der Pharma chem*. 2016; 8:61-66.
29. Senthil kumar S., Porkodi K., Gomathi R., Geetha A.M, Manonmani N. et al. Sol-gel derived silver doped nanocrystalline titania catalysed photodegradation of methylene blue from aqueous solution. *Journal of Dyes Pigments*; 2006; **69**: 22-30.
30. Tang W. Z. and An H., et al. UV/ $\text{TiO}_2$  photocatalytic oxidation of commercial dyes in aqueous solutions, *Chemosphere*, 1995;**31**:4157-4168.
31. Marye F. A , and Maria D.I. et al. Heterogeneous Photocatalysis. *Chem. Rev*. 1995; **83**: 341-350.
32. Poullos I. and Tsachpinis I., et al. Photodegradation of the textile dye reactive black 5 in the presence of semiconducting oxides, *J. Chem. Technol Biotechnol.*, 1999;**71**: 349-361.
33. Balaram K. A, Rao S., and Sreedhar B., et al. Synthesis, characterization and photocatalytic activity of alkaline earth metal doped titania, *Indian J. of Chemistry*, 2010;**49**:1189-1198.
34. Teshome A., Rao S., Subrahmanyam C. et al. Studies on Characterization and Photocatalytic Activities of Visible Light Sensitive  $\text{TiO}_2$  Nanocatalysts Co-doped with Magnesium and Copper. *International Research J. of Pure & Applied Chemistry*, 2011;**1(3)**: 84-81.